Synthesis, Characterization, and Photovoltaic Properties of Carbazole-Based Two-Dimensional Conjugated Polymers with Donor-π-Bridge-Acceptor Side Chains

ARTICLE *in* CHEMISTRY OF MATERIALS · NOVEMBER 2010

Impact Factor: 8.35 · DOI: 10.1021/cm1027157

8 AUTHORS, INCLUDING:

Hin-Lap Yip
South China University of Technology
125 PUBLICATIONS **6,880** CITATIONS
SEE PROFILE

Shengjian Liu
South China University of Technology
29 PUBLICATIONS **687** CITATIONS
SEE PROFILE

Alex K-Y Jen
University of Washington Seattle
391 PUBLICATIONS **15,909** CITATIONS
SEE PROFILE

6444 *Chem. Mater.* **2010,** *22,* 6444–6452
DOI:10.1021/cm1027157

CHEMISTRY OF MATERIALS
Article

Synthesis, Characterization, and Photovoltaic Properties of Carbazole-Based Two-Dimensional Conjugated Polymers with Donor-π-Bridge-Acceptor Side Chains

Chunhui Duan,[†] Kung-Shih Chen,[‡] Fei Huang,*[,†] Hin-Lap Yip,[‡] Shengjian Liu,[†] Jie Zhang,[†] Alex K.-Y. Jen,*[,‡] and Yong Cao[‡]

[†]*Institute of Polymer Optoelectronic Materials & Devices, Key Laboratory of Specially Functional Materials of the Ministry of Education, South China University of Technology, Guangzhou 510640, People's Republic of China, and* [‡]*Department of Materials Science and Engineering, University of Washington, Seattle, Washington 98195-2120, United States*

Received September 20, 2010. Revised Manuscript Received October 25, 2010

A series of carbazole-based narrow-band gap polymers with two-dimensional donor-π-bridge-acceptor (D-π-A) structures were synthesized and characterized for use in polymer bulk heterojunction solar cells. These D-π-A side-chain polymers were obtained through the Knoevenagel condensation between the aldehyde-containing precursor polymers and the corresponding acceptors. The resulting polymers have good solubility in common organic solvents and excellent thermal properties. The effects of the alkyl side chains and different dye contents on optical properties, electronic structures, charge-transporting ability, and device performance of these polymers were investigated. By blending these polymers as light-harvesting electron donors with (6,6)-phenyl-C_{71}-butyric acid methyl ester ($PC_{71}BM$) electron acceptors in bulk heterojunction solar cells, high power conversion efficiency (PCE), as high as 4.47%, could be achieved.

Introduction

Polymer bulk heterojunction (BHJ) solar cells have attracted considerable attention recently from both academic and industrial laboratories, because of their potential for low-cost, lightweight, printable, and flexible large-area devices.[1−6] Usually, the active content of a polymer BHJ solar cell is based on a blend of conjugated polymer donor and fullerene-derived acceptor that can phase-separate into nanometer-sized networks upon processing. To realize high power conversion efficiency (PCE), one of the most investigated approaches is to incorporate a narrow-band-gap (< 2.0 eV) conjugated polymer as an efficient electron donor to harvest light efficiently.[7−10] Over the past decade, several homopolymers, such as poly[2-methoxy-5-(3′,7′- dimethyloctyloxy)-*p*-phenylene-vinylene] (MDMO-PPV)[11] and regioregular poly(3-hexylthiophene) (P3HT),[12−15] have been extensively studied and the PCE of corresponding solar cells have reached efficiencies of 3%−5%. However, it is quite difficult to get any further improvements in solar cell performance from these homopolymers, because of their limited coverage of absorption in the solar spectrum and the small energy offset between the highest occupied molecular orbital (HOMO) of the donor and the lowest unoccupied molecular orbital (LUMO) of the acceptor that limits the magnitude of the short-circuit current (J_{sc}) and open-circuit voltage (V_{oc}), respectively.[16]

To optimize the light-harvesting material properties, conjugated polymers with alternating electron-rich (donor) and electron-deficient (acceptor) units copolymerized along their backbones have been vigorously explored, because their absorption and band gap can be readily tuned by controlling the intramolecular charge transfer (ICT) from donor to acceptor.[8−10] Based on this

*Authors to whom correspondence should be addressed. E-mails: msfhuang@scut.edu.cn, ajen@u.washington.edu.

(1) Yu, G.; Gao, J.; Hummelen, J. C.; Wudl, F.; Heeger, A. J. *Science* **1995**, *270*, 1789–1791.
(2) Gunes, S.; Neugebauer, H.; Sariciftci, N. S. *Chem. Rev.* **2007**, *107*, 1324–1338.
(3) Brabec, C. J.; Sariciftci, N. S.; Hummelen, J. C. *Adv. Funct. Mater.* **2001**, *11*, 15–26.
(4) Coakley, K. M.; McGehee, M. D. *Chem. Mater.* **2004**, *16*, 4533–4542.
(5) Thompson, B. C.; Frechet, J. M. J. *Angew. Chem., Int. Ed.* **2008**, *47*, 58–77.
(6) Helgesen, M.; Sondergaard, R.; Krebs, F. C. *J. Mater. Chem.* **2010**, *20*, 36–60.
(7) Kroon, R.; Lenes, M.; Hummelen, J. C.; Blom, P. W. M.; De Boer, B. *Polym. Rev.* **2008**, *48*, 531–582.
(8) Chen, J.; Cao, Y. *Acc. Chem. Res.* **2009**, *42*, 1709–1718.
(9) Cheng, Y. J.; Yang, S. H.; Hsu, C. S. *Chem. Rev.* **2009**, *109*, 5868–5923.
(10) Li, C.; Liu, M.; Pschirer, N. G.; Baumgarten, M.; Mullen, K. Chem. Rev. **2010**, DOI: 10.1021/cr100052z.
(11) Shaheen, S. E.; Brabec, C. J.; Sariciftci, N. S.; Padinger, F.; Fromherz, T.; Hummelen, J. C. *Appl. Phys. Lett.* **2001**, *78*, 841–843.
(12) Li, G.; Shrotriya, V.; Huang, J. S.; Yao, Y.; Moriarty, T.; Emery, K.; Yang, Y. *Nat. Mater.* **2005**, *4*, 864–868.
(13) Ma, W. L.; Yang, C. Y.; Gong, X.; Lee, K.; Heeger, A. J. *Adv. Funct. Mater.* **2005**, *15*, 1617–1622.
(14) Hau, S. K.; Yip, H. L.; Ma, H.; Jen, A. K. Y. *Appl. Phys. Lett.* **2008**, *93*, 233304.
(15) Yip, H. L.; Hau, S. K.; Baek, N. S.; Ma, H.; Jen, A. K. Y. *Adv. Mater.* **2008**, *20*, 2376–2382.
(16) Scharber, M. C.; Wuhlbacher, D.; Koppe, M.; Denk, P.; Waldauf, C.; Heeger, A. J.; Brabec, C. J. *Adv. Mater.* **2006**, *18*, 789–794.

Published on Web 11/08/2010

strategy, a series of narrow-band-gap donor−acceptor (D-A)-type conjugated polymers have been reported that show high performance with PCE values as high as ∼6%−7%.[17−30] Among them, the poly(*N*-alkyl-2,7-carbazole)s-based D−A copolymers exhibit outstanding photovoltaic performances, because of their excellent hole-transporting property and good stability of the carbazole units.[31,32] For example, the poly(*N*-alkyl-2,7-carbazole)s-based D-A copolymer poly[*N*-9′-heptadecanyl-2,7-carbazole-*alt*-5,5-(4′,7′-di-2-thienyl-2′,1′,3′-benzothia-diazole) (PCDTBT) developed by Leclerc et al. showed a PCE value of 3.6%.[21] Afterward, it was reported by Lee and Heeger et al. that the PCE of polymer BHJ solar cells based on PCDTBT can reach values as high as 6.1% when the devices were processed under optimized conditions, using [6,6]-phenyl-C_{71}-butyric acid methyl ester ($PC_{71}BM$) as the acceptor and titanium oxide as the optical spacer and hole-blocking layer.[33] Another carbazole-based polymer poly(2-(5-(5,6-bis(octyloxy)-4-(thiophen-2-yl)benzo[*c*]-[1,2,5]thiadiazol-7-yl)thiophen-2-yl)-9-octyl-9*H*-carbazole) (HXS-1) reported by Bo et al. also showed high PCE values (up to 5.4%).[30] Although the performance of D-A narrow-band-gap copolymer-based devices is quite promising, there is still a strong need for developing new polymer donors with optimized absorption, energy level, and charge mobility, to improve the PCE and stability of solar cells. However, most D-A copolymers reported so far are based on linearly alternating donor and acceptor units on the main chains. It has been shown that the variation of acceptors will dramatically affect the device performance, and it is very challenging to optimize the absorption, energy level, and charge mobility of the polymers simultaneously.[22,34]

Very recently, a new strategy was reported to develop narrow-band-gap conjugated polymers with a two-dimensional conjugated structure, where the electron acceptors are located at the end of the polymer side chains, instead of being on the main chain.[35,36] This new design is trying to take advantage of the well-established knowledge of dipolar chromophores to optimize the absorption and energy level of the resultant polymers.[37,38] Furthermore, their two-dimensional conjugated structure may enhance isotropic charge transport, which is very important for polymer BHJ solar cells.[39] Using this new design concept and the good charge-transporting properties of poly(*N*-alkyl-2,7-carbazole)s, a series of new poly(*N*-alkyl-2,7-carbazole) derivatives with different alkyl side chains and dye contents (see Scheme 1) have been designed and synthesized as potential candidates for high-efficiency polymer BHJ solar cells. The effect of the alkyl side chains and different dye contents on optical properties, electronic structures, charge-transporting ability, and device performance of the resultant polymers were investigated. All of these polymers exhibited promising photovoltaic properties, and the highest PCE achieved is more than 4% for EH-PCzDCN.

Experimental Section

General Details. All starting chemicals, unless otherwise specified, were purchased from Alfa Aesar or Sigma−Aldrich and used without further purification. Some solvents were distilled before use (tetrahydrofuran (THF) from sodium/benzopheone, acetonitrile from CaH_2, *N*,*N*-dimethylformamide (DMF) from $CaCl_2$, toluene that was washed with H_2SO_4 and then treated with $CaCl_2$). The other materials were common commercial level and used as received. ^1H and ^{13}C NMR spectra were recorded on a Bruker AV-300 (300 MHz) in deuterated chloroform solution. Number-average (M_n) and weight-average (M_w) molecular weights were determined by a Waters Model GPC 2410 chromatograph in THF, using a calibration curve with standard polystyrene as a reference. Differential scanning calorimetry (DSC) measurements were performed on a Netzsch Model DSC 204 system under N_2 flow at heating and cooling rates of 10 °C/min. UV−vis absorption spectra were recorded on an Hewlett−Packard Model HP 8453 spectrophotometer. Cyclic voltammetry (CV) was performed on a CHI Instruments Model CHI600D electrochemical workstation with a platinum working electrode and a platinum wire counter electrode at a scan rate of 50 mV/s against a Ag/Ag^+ (0.1 M of $AgNO_3$ in acetonitrile) reference electrode with a argon-saturated anhydrous

(17) Muhlbacher, D.; Scharber, M.; Morana, M.; Zhu, Z. G.; Waller, D.; Gaudiana, R.; Brabec, C. *Adv. Mater*. **2006**, *18*, 2884–2889.
(18) Wang, E. G.; Wang, L.; Lan, L. F.; Luo, C.; Zhuang, W. L.; Peng, J. B.; Cao, Y. *Appl. Phys. Lett*. **2008**, *92*, 033307.
(19) Coffin, R. C.; Peet, J.; Rogers, J.; Bazan, G. C. *Nat. Chem*. **2009**, *1*, 657–661.
(20) Hou, J.; Chen, H.-Y.; Zhang, S.; Li, G.; Yang, Y. *J. Am. Chem. Soc*. **2008**, *130*, 16144–16145.
(21) Blouin, N.; Michaud, A.; Leclerc, M. *Adv. Mater*. **2007**, *19*, 2295–2300.
(22) Blouin, N.; Michaud, A.; Gendron, D.; Wakim, S.; Blair, E.; Neagu-Plesu, R.; Belletete, M.; Durocher, G.; Tao, Y.; Leclerc, M. *J. Am. Chem. Soc*. **2008**, *130*, 732–742.
(23) Liang, Y.; Feng, D.; Wu, Y.; Tsai, S.-T.; Li, G.; Ray, C.; Yu, L. *J. Am. Chem. Soc*. **2009**, *131*, 7792–7799.
(24) Liang, Y. Y.; Xu, Z.; Xia, J. B.; Tsai, S. T.; Wu, Y.; Li, G.; Ray, C.; Yu, L. P. *Adv. Mater*. **2010**, *22*, E135–E138.
(25) Chen, H. Y.; Hou, J. H.; Zhang, S. Q.; Liang, Y. Y.; Yang, G. W.; Yang, Y.; Yu, L. P.; Wu, Y.; Li, G. *Nat. Photonics* **2009**, *3*, 649–653.
(26) Peet, J.; Kim, J. Y.; Coates, N. E.; Ma, W. L.; Moses, D.; Heeger, A. J.; Bazan, G. C. *Nat. Mater*. **2007**, *6*, 497–500.
(27) Wong, W. Y.; Wang, X. Z.; He, Z.; Djurisic, A. B.; Yip, C. T.; Cheung, K. Y.; Wang, H.; Mak, C. S. K.; Chan, W. K. *Nat. Mater*. **2007**, *6*, 521–527.
(28) Zou, Y. P.; Najari, A.; Berrouard, P.; Beaupre, S.; Aich, B. R.; Tao, Y.; Leclerc, M. *J. Am. Chem. Soc*. **2010**, *132*, 5330–5331.
(29) Piliego, C.; Holcombe, T. W.; Douglas, J. D.; Woo, C. H.; Beaujuge, P. M.; Frechet, J. M. J. *J. Am. Chem. Soc*. **2010**, *132*, 7595–7597.
(30) Qin, R.; Li, W.; Li, C.; Du, C.; Veit, C.; Schleiermacher, H.-F.; Andersson, M.; Bo, Z.; Liu, Z.; Inganas, O.; Wuerfel, U.; Zhang, F. *J. Am. Chem. Soc*. **2009**, *131*, 14612–14613.
(31) Li, J. L.; Dierschke, F.; Wu, J. S.; Grimsdale, A. C.; Mullen, K. *J. Mater. Chem*. **2006**, *16*, 96–100.
(32) Blouin, N.; Leclerc, M. *Acc. Chem. Res*. **2008**, *41*, 1110–1119.
(33) Park, S. H.; Roy, A.; Beaupre, S.; Cho, S.; Coates, N.; Moon, J. S.; Moses, D.; Leclerc, M.; Lee, K.; Heeger, A. J. *Nat. Photonics* **2009**, *3*, 297–303.
(34) Hou, J.; Park, M.-H.; Zhang, S.; Yao, Y.; Chen, L.-M.; Li, J.-H.; Yang, Y. *Macromolecules* **2008**, *41*, 6012–6018.
(35) Huang, F.; Chen, K.-S.; Yip, H.-L.; Hau, S. K.; Acton, O.; Zhang, Y.; Luo, J.; Jen, A. K. Y. *J. Am. Chem. Soc*. **2009**, *131*, 13886–13887.
(36) Duan, C. H.; Cai, W. Z.; Huang, F.; Zhang, J.; Wang, M.; Yang, T. B.; Zhong, C. M.; Gong, X.; Cao, Y. *Macromolecules* **2010**, *43*, 5262–5268.
(37) Marder, S. R.; Cheng, L. T.; Tiemann, B. G.; Friedli, A. C.; Blancharddesce, M.; Perry, J. W.; Skindhoj, J. *Science* **1994**, *263*, 511–514.
(38) Liu, S.; Haller, M. A.; Ma, H.; Dalton, L. R.; Jang, S. H.; Jen, A. K. Y. *Adv. Mater*. **2003**, *15*, 603–607.
(39) Roncali, J.; Leriche, P.; Cravino, A. *Adv. Mater*. **2007**, *19*, 2045–2060.

Scheme 1. Structures of the Polymers

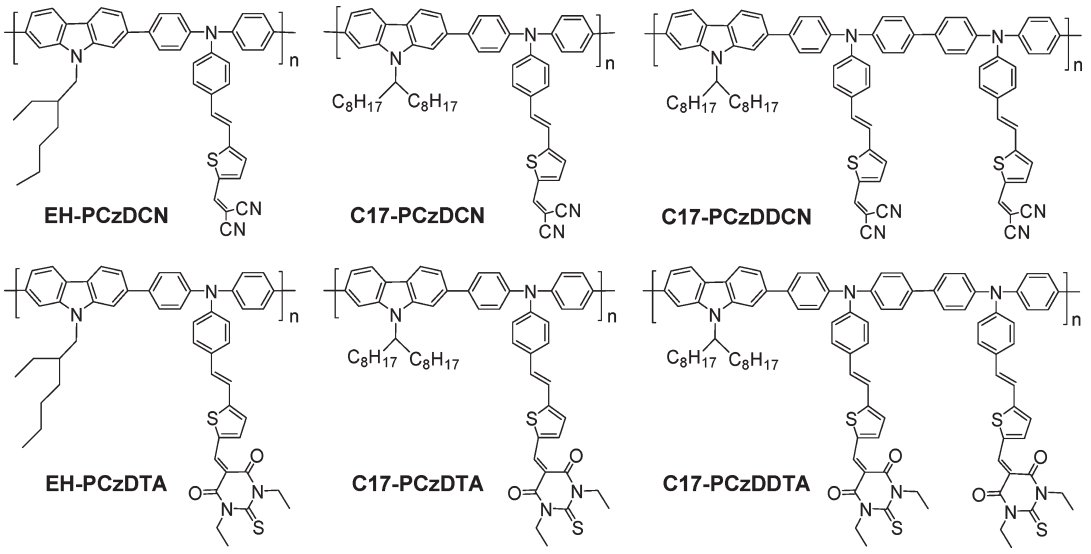

solution of 0.1 mol/L tetrabutylammonium hexafluorophosphate (Bu_4NPF_6) in acetonitrile. The polymer films for electrochemical measurements were coated from a polymer−THF dilute solution.

Solar Cell Device Fabrication and Characterization. Indium tin oxide (ITO)-coated glass substrates (15 Ω per square) were cleaned sequentially via sonication in detergent, deionized water, acetone, and isopropyl alcohol, and then dried in a nitrogen stream, followed by an oxygen plasma treatment. To fabricate photovoltaic devices, a thin layer (ca. 40 nm) of PEDOT:PSS (Baytron P VP AI 4083, filtered at 0.45 μm) was first spin-coated on the precleaned ITO-coated glass substrates at 5000 rpm and baked at 140 °C for 10 min under ambient conditions. The substrates were then transferred into an argon-filled glovebox. Subsequently, the polymer:$PC_{71}BM$ active layer (ca. 80 nm) was spin-coated on the PEDOT:PSS layer at 1000 rpm from a homogeneously blended solution. The solution was prepared by dissolving the polymer (5 mg/mL) and $PC_{71}BM$ (20 mg/mL) in 1,2-dichlorobenzene and then was filtered with a 0.2 μm poltetrafluoroethylene (PTFE) filter. The substrates were annealed at 150 °C for 10 min prior to electrode deposition. At the final stage, the substrates were pumped down to high vacuum ($< 2 \times 10^{-6}$ Torr), and calcium (10 nm) topped with aluminum (100 nm) was thermally evaporated onto the active layer through shadow masks to define the active area of the devices. A curled metal wire was gently tapped on the metal electrode when making connection to the testing equipment without scratching the metal electrode.

The current density−voltage ($J-V$) characteristics of photovoltaic devices were measured under ambient conditions, using a Keithley Model 2400 source-measurement unit. An Oriel xenon lamp (450 W) with an AM 1.5 G filter was used as the solar simulator. The light intensity was calibrated to 100 mW/cm^2, using a calibrated silicon cell with a KG5 filter, which is traced to the National Renewable Energy Laboratory (NREL). External quantum efficiency (EQE) measurements were taken using a monochromator (Newport, Model Cornerstone 130) that was joined to the same xenon lamp and a lock-in amplifier (Stanford Research Systems, Model SR 830) coupled to a light chopper.

Atomic Force Microscope. Atomic force microscopy (AFM) images were obtained using a Veeco multimode AFM microscope with a Nanoscope III controller under tapping mode.

Field-Effect Transistor (FETs). Top contact organic field-effect transistors (FETs) were fabricated on heavily *n*-doped silicon substrates with a 300-nm-thick thermally grown SiO_2 dielectric (from Montco Silicon Technologies, Inc.). Before organic semiconductor deposition, the substrates were treated with hexamethyldisilazane (HMDS) via vapor-phase deposition in a vacuum oven (200 mTorr, 100 °C, 3 h). The organic semiconductor films were spin-coated in a dry nitrogen environment from a 5 mg mL^{-1} chloroform solution. Interdigitated source and drain electrodes (L = 80 μm, W = 9600 μm, W/L = 120) were defined by evaporating a 50-nm-thick gold film through a shadow mask from a resistively heated Mo boat at 3×10^{-6} Torr. FETs characterization was carried out under nitrogen using an Agilent Model 4155B semiconductor parameter analyzer. The field-effect mobility was calculated in the saturated regime from derivative plots of the square root of the source-drain current versus gate voltage.

Synthesis. 4,4′-Bis[(*p*-bromophenyl)phenylamino]biphenyl (**1**),[40] diethyl (2-methylthiophene)-phosphonate,[41] *N*-(2-ethylhexyl)-2,7-bis(4,4,5,5-tetramethyl-1,3,2-dioxaborolane-2-yl)carbazole (**M1**),[42] *N*-(9-heptadecanyl)-2,7-bis(4,4,5,5-tetramethyl-1,3,2-dioxaborolane-2-yl)carbazole (**M3**),[21] and 2-[2-[4-[*N*,*N*-di(4-bromophenyl)amino]-phenyl] ethenyl] thien-5-al (**M2**)[35] were prepared according to reported methods.

4,4′-Bis[(*p*-formylphenyl)phenylamino]biphenyl (2). $POCl_3$ (50 mL, 536 mmol) was added dropwise to a solution of compound **1** (10 g, 15.5 mmol) in 50 mL of dry DMF at 0 °C. The reaction mixture was allowed to warm to 50 °C and stirred for 2 h. After cooling to room temperature, the mixture was poured into water, neutralized with sodium carbonate, and extracted with dichloromethane. The combined organic phases were washed with water and brine and dried over magnesium sulfate, and the solvent was removed under reduced pressure. The residue was purified using column chromatography (silica gel, petroleum ether/dichloromethane (3/1)) to yield 7.2 g (66%) of compound **2**. ^{1}H NMR ($CDCl_3$, ppm): 9.87 (s, 2H), 7.74−7.71 (d, 4H), 7.55−7.52 (d, 4H), 7.47−7.45 (d, 4H), 7.22−7.18 (d, 4H), 7.09−7.06 (m, 8H). ^{13}C NMR ($CDCl_3$, ppm): 190.42, 152.65, 145.27, 145.19, 136.86, 132.89, 131.39, 129.95, 128.14, 127.53, 126.20, 120.37, 117.94. Anal. Calcd. for ($C_{38}H_{26}Br_2N_2O_2$) (%): C, 64.96; H, 3.704; N, 3.987. Found (%): C, 62.98; H, 3.541; N, 3.793.

(40) Li, J. F.; Marks, T. J. *Chem. Mater.* **2008**, *20*, 4873–4882.
(41) Lee, W.-H.; Kong, H.; Oh, S.-Y.; Shim, H.-K.; Kang, I.-N. *J. Polym. Sci., Part A: Polym. Chem.* **2009**, *47*, 111–120.
(42) Dierschke, F.; Grimsdale, A. C.; Mullen, K. *Macromol. Chem. Phys.* **2004**, *205*, 1147–1154.

4,4′-Bis[(*p*-(2-thienylethenyl)phenyl)phenylamino]biphenyl (3). To a solution of 7.0 g (10 mmol) of compound **2** and 5.2 g (22.0 mmol) of diethyl (2-methylthiophene)-phosphonate in 80 mL of dry THF was added 22.0 mL of 1 M potassium *tert*-butoxide methanol solution. The reaction mixture was stirred overnight at room temperature and then was diluted with dichloromethane and water. The two phases were separated, and the water phase was extracted twice with dichloromethane. The combined organic extracts were washed three times with water, dried over magnesium sulfate, concentrated under reduced pressure, and purified with column chromatography (silica gel, petroleum ether/dichloromethane (3/1)) to give 7.5 g of yellowish compound **3** with a yield of 87%. ^{1}H NMR ($CDCl_3$, ppm): 7.46 (d, 4H), 7.35 (d, 8H), 7.18−7.12 (m, 8H), 7.08−7.00 (m, 12H), 6.91(d, 2H). ^{13}C NMR ($CDCl_3$, ppm): 146.58, 146.52, 146.09, 143.11, 135.36, 132.33, 131.91, 130.00, 127.66, 127.62, 127.58, 127.32, 125.76, 125.67, 124.59, 124.06, 120.67, 115.45. Anal. Calcd. for ($C_{48}H_{34}Br_2N_2S_2$) (%): C, 66.82; H, 3.944; N, 3.248; S, 7.425. Found (%): C, 65.96; H, 3.752; N, 3.127; S, 6.624.

4,4′-Bis[(*p*-(5-formyl-2-thienylethenyl)phenyl)phenylamino]biphenyl (M4). Compound **3** (7.0 g, 8.1 mmol) was dissolved in 50 mL of dry DMF. $POCl_3$ (30 mL, 322 mmol) was added dropwise to the mixture at 0 °C. The reaction mixture was allowed to warm to 50 °C and stirred for 2 h. After cooling to room temperature, the mixture was poured into water, neutralized with sodium carbonate, and extracted with dichloromethane. The combined organic phases were washed with water and brine and then dried over magnesium sulfate, and the solvent was removed under reduced pressure. The crude product was purified using column chromatography (silica gel, petroleum ether/dichloromethane (2/1)) to yield 4.9 g (66%) of monomer **M4**. ^{1}H NMR ($CDCl_3$, ppm): 9.84 (s, 2H), 7.73−7.71 (d, 2H), 7.50−7.47 (d, 4H), 7.40−7.37 (m, 8H), 7.16−7.00 (m, 18H). ^{13}C NMR ($CDCl_3$, ppm): 182.52, 152.90, 147.76, 146.20, 145.88, 141.18, 137.37, 135.69, 132.48, 132.33, 130.32, 130.04, 128.06, 127.71, 126.14, 124.96, 123.35, 119.32, 116.09. Anal. Calcd. for ($C_{48}H_{34}Br_2N_2S_2$) (%): C, 65.36; H, 3.704; N, 3.050; S, 6.972. Found (%): C, 65.00; H, 3.436; N, 3.025; S, 6.002.

EH-PCzCHO. In a 50-mL two-necked round-bottomed flask, 531 mg (1.0 mmol) of monomer **M1**, 539 mg (1.0 mmol) of **M3**, and 10 mg of $Pd(PPh_3)_4$ were dissolved in a mixture of 10 mL of degassed toluene, 10 mL of distilled THF and 4 mL of degassed aqueous sodium carbonate (2.0 M). The solution was flushed with argon for 15 min. The mixture was refluxed with vigorous stirring in darkness for 24 h under an argon atmosphere. After cooling to room temperature, the mixture was poured into methanol. The precipitated material was collected by filtration through a funnel. After washing with acetone for 24 h in a Soxhlet apparatus to remove oligomers and catalyst residues, the resulting material was dissolved in 30 mL of chloroform. The solution was filtered with a 0.45-μm PTFE filter, concentrated, and precipitated from methanol to yield EH-PCzCHO as an orange solid (387 mg, 59%). ^{1}H NMR ($CDCl_3$, ppm): 9.85 (s, 1H), 8.16−8.13 (m, 2H), 7.70−7.64 (m, 5H), 7.59−7.56 (m, 2H), 7.51−7.40 (m, 4H), 7.33−7.31 (m, 3H), 7.22−7.20 (m, 2H), 7.14- 7.12 (m, 4H), 4.26 (m, 2H), 2.16 (m, 1H), 1.45−1.28 (m, 8H), 0.97−0.86 (m, 6H). GPC (THF, polystyrene standard): M_n = 2.7 kg/mol, M_w = 7.1 kg/mol, PDI = 2.6.

EH-PCzDCN. Pyridine (0.5 mL) was added to a solution of EH-PCzCHO (100 mg, 0.15 mmol of the repeating unit) and malononitrile (396 mg, 6.0 mmol) in 10 mL of chloroform. The mixture solution was stirred in darkness for 36 h at room temperature, after which the resulting mixture was poured into methanol and the precipitate was filtered off. The resulted polymer was dissolved in 15 mL of chloroform. The solution was filtered through a 0.45-μm PTFE filter, concentrated, and precipitated from methanol to yield the polymer as a black solid (88 mg, 83%). ^{1}H NMR ($CDCl_3$, ppm): 8.14−8.10 (m, 2H), 7.72−7.65 (m, 5H), 7.59−7.56 (m, 3H), 7.50−7.41 (m, 4H), 7.33−7.31 (m, 3H), 7.22−7.20 (m, 3H), 7.13−7.07 (m, 3H), 4.26 (m, 2H), 2.17 (m, 1H), 1.44−1.26 (m, 8H), 0.96−0.86 (m, 6H). GPC (THF, polystyrene standard): M_n = 2.7 kg/mol, M_w = 7.3 kg/mol, PDI = 2.7.

EH-PCzDTA. Pyridine (0.5 mL) was added to a solution of EH-PCzCHO (100 mg, 0.15 mmol of the repeating unit) and 1, 3-diethyl-2-thiobarbituric acid (600 mg, 3 mmol) in 10 mL of chloroform. The mixture solution was stirred in darkness for 36 h at room temperature, after which the resulting mixture was poured into methanol and the precipitate was filtered off. The resulted polymer was dissolved in 15 mL of chloroform. The solution was filtered through a 0.45-μm PTFE filter, concentrated, and precipitated from methanol to yield the polymer as a black solid (101 mg, 81%). ^{1}H NMR ($CDCl_3$, ppm): 8.63 (s, 1H), 8.15−8.12 (m, 2H), 7.81−7.80 (m, 1H), 7.71−7.66 (m, 4H), 7.59−7.57 (m, 2H), 7.51−7.40 (m, 4H), 7.34−7.31 (m, 3H), 7.24−7.16 (m, 4H), 7.13−7.08 (m, 2H), 4.64−4.57 (m, 4H), 4.27 (m, 2H), 2.18 (m, 1H), 1.44−1.24 (m, 14H), 0.97−0.86 (m, 6H). GPC (THF, polystyrene standard): M_n = 2.7 kg/mol, M_w = 6.1 kg/mol, PDI = 2.3.

C17-PCzCHO. C17-PCzCHO was synthesized according to a procedure similar to that for EH-PCzCHO with respective monomers. ^{1}H NMR ($CDCl_3$, ppm): 9.86 (s, 1H), 8.16−8.13 (m, 2H), 7.79−7.62 (m, 7H), 7.47−7.41 (m, 4H), 7.34−7.32 (d, 3H), 7.24−7.22 (d, 2H), 7.15−7.07 (m, 4H), 4.69 (s, 1H), 2.38 (m, 2H), 2.00 (m, 2H), 1.27−1.15 (m, 24H), 0.82 (t, 6H). GPC (THF, polystyrene standard): M_n = 7.9 kg/mol, M_w = 15.5 kg/mol, PDI = 2.0.

C17-PCzDCN. C17-PCzDCN was synthesized according to a procedure similar to that for EH-PCzDCN. ^{1}H NMR ($CDCl_3$, ppm): 8.15 (s, 2H), 7.77−7.60 (m, 8H), 7.47−7.44 (m, 4H), 7.34−7.32 (m, 3H), 7.25−7.15 (m, 6H), 4.68 (s, 1H), 2.40 (m, 2H), 2.00 (m, 2H), 1.26−1.14 (m, 24H), 0.79 (t, 6H). GPC (THF, polystyrene standard): M_n = 7.4 kg/mol, M_w = 12.5 kg/mol, PDI = 1.7.

C17-PCzDTA. C17-PCzDTA was synthesized according to a procedure similar to that for EH-PCzDTA. ^{1}H NMR ($CDCl_3$, ppm): 8.63 (s, 1H), 8.16 (s, 2H), 7.78−7.61 (m, 7H), 7.47−7.39 (m, 4H), 7.35−7.32 (m, 3H), 7.26−7.16 (m, 6H), 4.60−4.58 (m, 5H), 2.37 (m, 2H), 1.99 (m, 2H), 1.79 (t, 6H), 1.26−1.14 (m, 24H), 0.80 (t, 6H). GPC (THF, polystyrene standard): M_n = 5.6 kg/mol, M_w = 6.7 kg/mol, PDI = 1.2.

C17-PCzDCHO. C17-PCzDCHO was synthesized according to a procedure similar to that for EH-PCzCHO with respective monomers. ^{1}H NMR ($CDCl_3$, ppm): 9.90 (s, 2H), 8.16 (m, 2H), 7.70−7.47 (m, 18H), 7.31−7.26 (m, 6H), 7.17−7.00 (m, 12H), 4.70 (m, 1H), 2.39 (m, 2H), 2.00 (m, 2H), 1.17−1.01 (m, 24H), 0.82 (t, 6H). GPC (THF, polystyrene standard): M_n = 13.1 kg/mol, M_w = 29.4 kg/mol, PDI = 2.3.

C17-PCzDDCN. C17-PCzDDCN was synthesized according to a procedure similar to that for EH-PCzDCN. ^{1}H NMR ($CDCl_3$, ppm): 8.14 (s, 2H), 7.73 (s, 2H), 7.68−7.45 (m, 18H), 7.31−7.26 (m, 6H), 7.17−7.00 (m, 12H), 4.68 (m, 1H), 2.39 (m, 2H), 2.00 (m, 2H), 1.17−1.01 (m, 24H), 0.82 (t, 6H). GPC (THF, polystyrene standard): M_n = 13.7 kg/mol, M_w = 27.2 kg/mol, PDI = 2.0.

C17-PCzDDTA. C17-PCzDDTA was synthesized according to a procedure similar to that for EH-PCzDTA. ^{1}H NMR

Scheme 2. Synthetic Route of the Monomers and Polymers

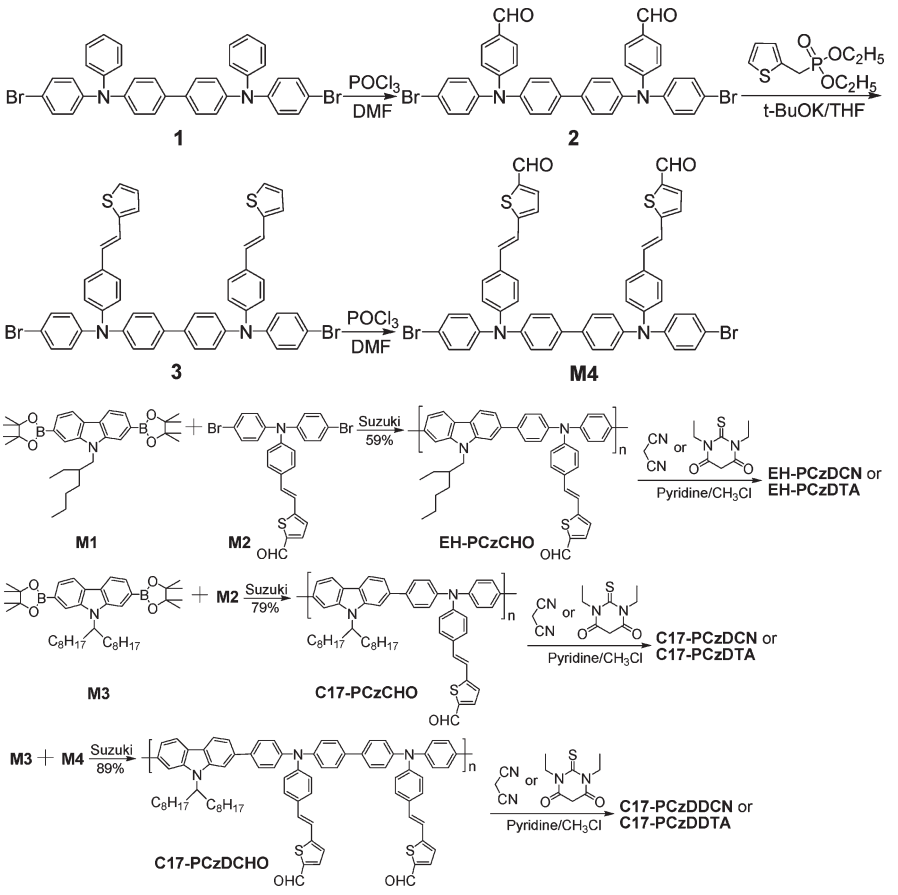

($CDCl_3$, ppm): 8.61 (d, 2H), 8.10 (m, 2H), 7.59−7.42 (m, 24H), 7.17−7.00 (m, 12H), 4.57 (m, 9H), 2.34 (m, 2H), 2.17 (m, 2H), 1.62 (12H), 1.25−1.12 (m, 24H), 0.78 (t, 6H). GPC (THF, polystyrene standard): M_n = 8.4 kg/mol, M_w = 11.6 kg/mol, PDI = 1.4.

Results and Discussion

Synthesis and Characterization. The synthetic route of making new monomer **M4** and target polymers is outlined in Scheme 2. The monomers **M1**, **M2**, and **M3** were prepared according to the reported methods.[21,35,42] The new monomer **M4** was prepared from compound **1** via a three-step process. Vilsmeier−Haack formylation of the arylamine compound **1** was used initially to prepare the crucial intermediate **2** under mild conditions to afford a moderate yield of 66%. After purification via column chromatography, aldehyde **2** was reacted with diethyl (2-methylthiophene)-phosphonate in THF, using the Wittig−Horner reaction to afford **3** with a high yield of 87%. The resultant aldehyde-functionalized monomer **M4** was obtained by Vilsmeier−Haack formylation of **3** with conditions similar to those used for compound **2**. The polymerizations for three aldehyde-functionalized precursor polymers—EH-PCzCHO, C17-PCzCHO, and C17-PCzDCHO—were carried out via Suzuki polycondensation reaction with equimolar amounts of the corresponding monomers. The conditions for these polymerizations were almost identical (0.1 M total monomer concentration, ~0.9 mol % catalyst, refluxing in the mixture solvents of toluene/THF and 2.0 M aqueous sodium carbonate, argon atmosphere, reaction time of 24 h). The target two-dimensional narrow-band-gap polymers EH-PCzDCN, EH-PCzDTA, C17-PCzDCN, C17-PCzDTA, C17-PCzDDCN, and C17-PCzDDTA were obtained by reacting the aldehyde-containing precursor polymers with malononitrile or diethylthiobarbituric acid, respectively, using the Knoevenagel condensation in the presence of pyridine to afford a high yield (see Table 1). The efficient acceptor conversion were verified by the complete disappearance of the aromatic aldehyde proton signal at ~9.85 ppm and the appearance of olefinic proton signal at ~7.75 ppm for three malononitrile-functionalized polymers and ~8.62 ppm for three diethylthiobarbituric acid-functionalized polymers.[36,43] This way, the entire band gap of the resulting polymers can be readily controlled using malononitrile or diethylthiobarbituric acid acceptors. Compared to C17-PCzDCN and C17-PCzDTA, EH-PCzDCN and EH-PCzDTA have shorter alkyl side chains, whereas C17-PCzDDCN and C17-PCzDDTA have higher dye contents. Thus, the impact of different alkyl chains and dye contents on optical properties, electronic structures, charge-transporting ability, and device performance of these polymers can be systematically investigated. Molecular weight and molecular-weight distributions of the polymers were determined by gel

(43) Zhang, Z.-G.; Zhang, K.-L.; Liu, G.; Zhu, C.-X.; Neoh, K.-G.; Kang, E.-T. *Macromolecules* **2009**, *42*, 3104–3111.

Table 1. Reaction Yields, Molecular Weights, and Thermal Properties of the Polymers

polymer	yield (%)	M_w (kg/mol)	PDI	T_g (°C)
EH-PCzDCN	83	7.3	2.7	182
EH-PCzDTA	81	6.1	2. 3	189
C17-PCzDCN	83	12.5	1.7	166
C17-PCzDTA	95	6.7	1.2	163
C17-PCzDDCN	91	27.2	2.0	-
C17-PCzDDTA	95	11.6	1.4	-

permeation chromatography (GPC) against the polystyrene standard, with THF as an eluent, and the results are listed in Table 1. All of the resulting polymers have good solubility in common organic solvents (THF, chloroform, toluene, chlorobenzene, *o*-dichlorobenzene, etc.) and good processing ability to form uniform thin films.

Thermal Properties. The thermal transitions of these polymers were investigated by DSC. After thermal annealing upon heating to 250 °C, four of the six resultant polymers (EH-PCzDCN, EH-PCzDTA, C17-PCzDCN, and C17-PCzDTA) exhibited relatively high glass-transition temperature (T_g) values, ranging from 163 °C to 189 °C, as depicted in Table 1. Only glass transitions could be observed with no crystallization or melting peak upon further heating beyond the T_g value for them. Interestingly, C17-PCzDDCN and C17-PCzDDTA did not reveal any clear T_g values, despite various DSC measurements being performed. The high T_g value suggests that the thermal stability of these polymers is adequate to retard the deformation of the active layer morphology at elevated temperatures, which is desirable for polymer BHJ solar cell devices.[44]

Optical Properties. The absorption spectra of polymer thin films, spin-coated onto quartz substrates, are shown in Figure 1. It can be observed that all of the polymers show two obvious absorption peaks. Their first absorption peak of these polymers is observed at ~380 nm, which corresponds to the $\pi-\pi^*$ transition of their conjugated main chains.[35,36,43] Their broad absorption band at longer wavelengths can be attributed to the strong ICT interaction between their conjugated backbone and the pendant acceptor groups.[35,36,43,45,46] An obviously red-shifted ICT absorbance peak could be observed by changing the pendant acceptor groups from malononitrile to diethylthiobarbituric acid for polymers with the same main chains, because of the more-intense ICT interaction in diethylthiobarbituric acid-functionalized polymers than malononitrile-functionalized polymers. Clearly, the polymers C17-PCzDDCN and C17-PCzDDTA, which have a higher dye content in each repeat unit than their monodye-containing analogues C17-PCzDTA and C17-PCzDTA, show more-intense and broad absorption at the long wavelength band. More interesting, a slightly red-shifted ICT absorption peak for didye-containing polymer, compared with their monodye-containing analogues,

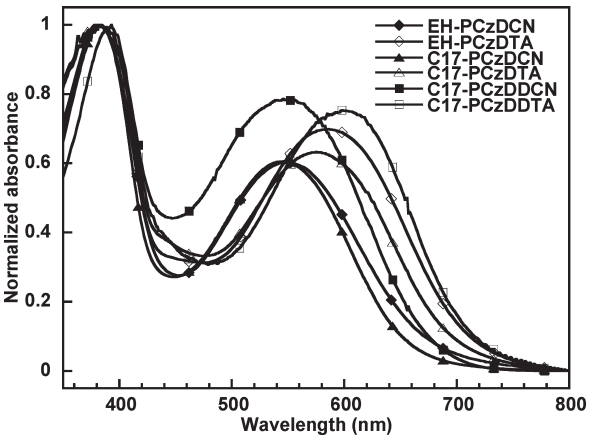

Figure 1. UV−vis spectra of the polymers in solid state.

Table 2. Optical and Electrochemical Properties of the Polymers

polymer	λ_{abs} (nm)	E_g^{opt} (eV)	E_{ox} (V)	E_{HOMO} (eV)	E_{LUMO} (eV)
EH-PCzDCN	380,548	1.83	0.80	−5.23	−3.40
EH-PCzDTA	382,586	1.74	0.82	−5.25	−3.51
C17-PCzDCN	382,545	1.88	0.86	−5.29	−3.41
C17-PCzDTA	384,575	1.77	0.87	−5.30	−3.53
C17-PCzDDCN	382,546	1.83	0.77	−5.20	−3.37
C17-PCzDDTA	393,598	1.74	0.81	−5.24	−3.50

could also be observed, especially for C17-PCzDDTA, for which both absorption peaks exhibit large red-shifts, compared to C17-PCzDTA. In addition, the alkyl side chain on the conjugated polymer backbone can also influence the optical properties of the polymer with the same main chain. There is a slightly red-shifted and broadened absorption peak of ethylhexyl-substituted EH-PCzDCN and EH-PCzDTA, compared to their heptadecanyl-substituted counterparts C17-PCzDCN and C17-PCzDTA, respectively, which could be explained by smaller steric hindrance between alkyl side chains and conjugated backbone of EH-PCzDCN and EH-PCzDTA than that of C17-PCzDCN and C17-PCzDTA, and consequently show more effective packing. The optical property data of the polymers are listed in Table 2. As discussed previously, the easily tuned optical properties and energy gaps of these six polymers indicate that it is possible to combine two-dimensional molecular design and good hole-transporting properties of carbazole, leading to the development of efficient materials for polymer BHJ solar cells applications.

Electrochemical Properties. To obtain the band diagram of the polymers, and consequently understand the relationship between the energy levels of the materials and the performance of the resulting solar cell devices, we conducted electrochemical experiments using cyclic voltammetry (CV) to calculate the energy levels of the HOMO and LUMO of the polymers. The oxidation potentials that are generally used to estimate the HOMO levels of the polymers were determined via CV, using a platinum electrode and a Ag/Ag^+ (0.1 M of $AgNO_3$ in acetonitrile) electrode as the work electrode and the reference electrode, respectively, in a 0.1 M Bu_4NPF_6 acetonitrile solution at a scan rate of 50 mV/s. As shown in Figure 2, all polymers show two quasi-reversible oxidative

(44) Li, J. Y.; Liu, D.; Li, Y. Q.; Lee, C. S.; Kwong, H. L.; Lee, S. T. *Chem. Mater*. **2005**, *17*, 1208–1212.
(45) Leriche, P.; Frere, P.; Cravino, A.; Aleveque, O.; Roncali, J. *J. Org. Chem*. **2007**, *72*, 8332–8336.
(46) Tang, Z.-M.; Lei, T.; Wang, J.-L.; Ma, Y.; Pei, J. *J. Org. Chem*. **2010**, *75*, 3644–3655.

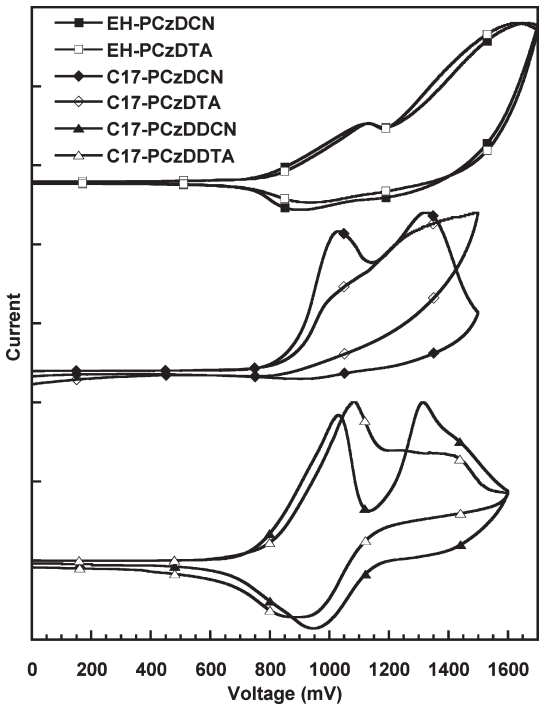

Figure 2. Cyclic voltammograms of the polymer films.

waves in the positive potential range from 0 mV to 1600 mV. The first one is attributed to the oxidation of the triphenylamine unit, and the other one may be due to the oxidation of the carbazole moiety.[43] The HOMO energy levels of the polymers were obtained from their oxidation potential, using the ferrocence value of 4.8 eV below the vacuum as the internal standard.[47] Hence, the HOMO levels energy levels could be calculated from the equation

$$E_{\mathrm{HOMO}}\ (\mathrm{eV}) = -e(E_{\mathrm{ox}} + 4.43)$$

where E_{ox} is the onset oxidation potential of the polymers vs Ag/Ag^{+}. The HOMO energy levels values of the resultant polymers were estimated to range from −5.20 eV to −5.30 eV. Note that the reductive curves of the polymers could hardly be obtained. Therefore, the LUMO energy levels values of the polymers were estimated from their optical band gaps and HOMO energy levels values, using the equation

$$E_{\mathrm{LUMO}} = E_{\mathrm{HOMO}} + E_{\mathrm{g}}^{\mathrm{opt}}$$

where $E_{\mathrm{g}}^{\mathrm{opt}}$ denotes the optical band gaps of the polymers. The HOMO and LUMO energy levels values are outlined in Table 2.

Obviously, the HOMO energy levels of the polymers with similar conjugated main chains have little change, despite the presence of different pendant acceptor groups, while their LUMO are mainly determined by the acceptor on the side chains. The phenomenon is consistent with the results of other reported two-dimensional D-π-A conjugated polymers[35,36,43] and triphenylamine-based small molecular solar cell materials.[45,48] The relatively low HOMO levels of the resultant polymers are advantageous for getting higher V_{oc} in solar cell devices,[25] because V_{oc} is related to the offset between the HOMO levels of donor materials and the LUMO levels of acceptor materials.[16] Moreover, the LUMO levels of the polymers are still much higher than those of (6,6)-phenyl-C_{61}-butyric acid methyl ester (PCBM) or $PC_{71}BM$, which indicates that charge transfer from the polymers to PCBM or $PC_{71}BM$ would be allowed.[49,50]

Photovoltaic Properties. Polymer BHJ solar cells using the six polymers as electron-donor materials were fabricated with devices whose structures consist of ITO/poly-(3,4-ethylenedioythiophene):poly(styrene sulfonic acid) (PEDOT:PSS)/polymer:$PC_{71}BM$/Ca/Al. After spin-coating a 40-nm layer of PEDOT:PSS onto precleaned ITO substrates, the polymer:$PC_{71}BM$ (1:4, w:w) solution in 1,2-dichlorobenzene was spin-coated, then the samples were annealed at 150 °C for 10 min. Finally, the devices were completed with the deposition of a Ca (10 nm)/Al (100 nm) cathode under high vacuum. $PC_{71}BM$ was used as electron-acceptor materials, because it has similar electronic properties to PCBM, but a much stronger absorption in the visible region with a broad peak from 440 nm to 530 nm, which can complement the absorption valley of the polymers (see Figures 1 and 3).[51] The resultant photovoltaic cells were then tested under ambient conditions using a Keithley Instruments Model 2400 source-measurement unit and an Oriel xenon lamp (450 W) with an AM1.5 filter. The light intensity was calibrated to 100 mW/cm^2, using a calibrated standard silicon solar cell with a KG5 filter, which is traced to the National Renewable Energy Laboratory (NREL). The performances of all polymers and typical $J-V$ curves, demonstrating the behavior of the devices, are presented in Table 3 and Figure 4, respectively.

Certain trends could be observed from the results of the photovoltaic characterization. First, the V_{oc} of the solar cells decreased as the dye contents in the polymers increased, which is relevant to the HOMO levels of the polymers. However, the alkyl side chains have little influence on the V_{oc} of the solar cells based on the polymers with the same main chains. Second, the bulky side chain of the polymers leads to a significant decrease in J_{sc} and FF and, consequently, a decrease in the PCE of the solar cells. For instance, the J_{sc}, FF, and average PCE values of EH-PCzDCN are 8.94 mA/cm^2, 0.51, and 4.16%, respectively; however, the values of those same parameters for C17-PCzDCN decreased to 7.51 mA/cm^2, 0.44, and 2.91%, respectively, while they have the same V_{oc} value (0.91 V).

Interestingly, some of the polymers exhibit promising photovoltaic properties, despite the fact that no extensive optimization work has been performed. The best performing

(47) Pommerehne, J.; Vestweber, H.; Guss, W.; Mahrt, R. F.; Bassler, H.; Porsch, M.; Daub, J. *Adv. Mater.* **1995**, *7*, 551–554.
(48) Roquet, S.; Cravino, A.; Leriche, P.; Aleveque, O.; Frere, P.; Roncali, J. *J. Am. Chem. Soc.* **2006**, *128*, 3459–3466.
(49) Sariciftci, N. S.; Smilowitz, L.; Heeger, A. J.; Wudl, F. *Science* **1992**, *258*, 1474–1476.
(50) Kraabel, B.; McBranch, D.; Sariciftci, N. S.; Moses, D.; Heeger, A. J. *Phys. Rev. B* **1994**, *50*, 18543.
(51) Yao, Y.; Shi, C.; Li, G.; Shrotriya, V.; Pei, Q.; Yang, Y. *Appl. Phys. Lett.* **2006**, *89*, 153507.

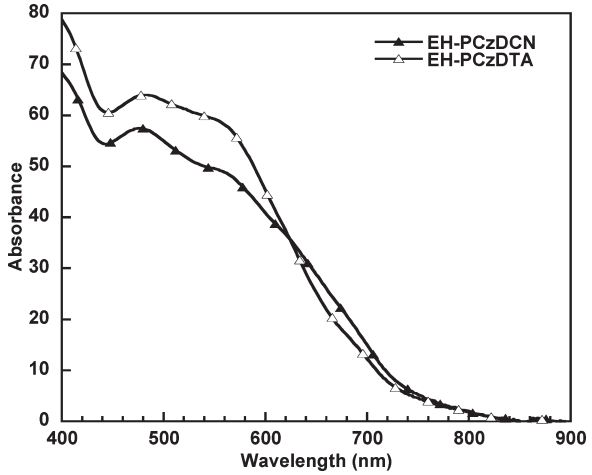

Figure 3. UV−vis absorption spectra of polymer:$PC_{71}BM$ (1:4, w:w) blend films.

Table 3. Photovoltaic Performance of the Polymers Measured under the Illumination of Simulated AM 1.5 G Conditions (100 mW/cm^2)

polymer	V_{oc} (V)	J_{sc} (mA/cm^2)	FF	PCE (%)
EH-PCzDCN	0.91	8.94	0.51	4.16
EH-PCzDTA	0.92	8.18	0.47	3.52
C17-PCzDCN	0.91	7.51	0.44	2.91
C17-PCzDTA	0.89	6.23	0.38	2.09
C17-PCzDDCN	0.83	7.18	0.39	2.34
C17-PCzDDTA	0.84	6.53	0.40	2.19

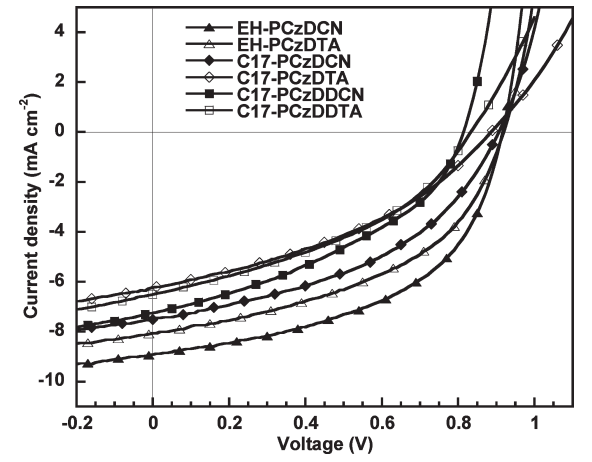

Figure 4. $J-V$ curves of the solar cells based on the polymers under illumination of AM 1.5G (light intensity = 100 mW/cm^2).

devices are based on EH-PCzDCN, which showed a maximum PCE of 4.47% and an average PCE of 4.16%. Note that all of the solar cells have large V_{oc} values (>0.8 eV), because of the relatively low HOMO levels of their active donor polymers. The other polymers also exhibited moderate photovoltaic properties, and higher PCE values can also be expected if more insightful optimization were to be performed, considering their excellent optical properties and electronic structures.

The external quantum efficiency (EQE) of the solar cells illuminated by monochromatic light was determined to provide insightful understanding of the photovoltaic properties of the resulting polymers. As shown by the EQE curves presented in Figure 5, all of the polymers

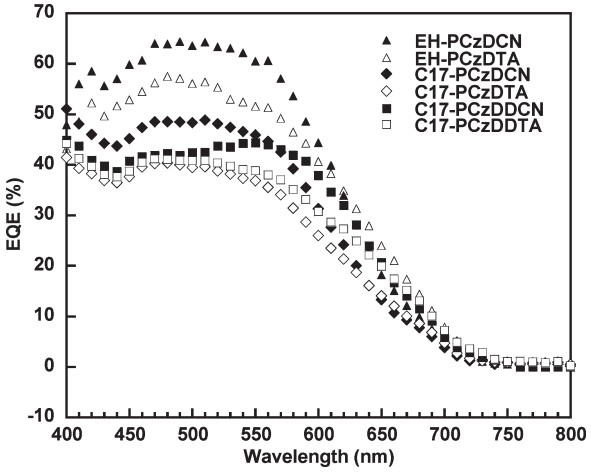

Figure 5. EQE spectra of the solar cell devices prepared from the polymer:$PC_{71}BM$ (1:4, w-w) mixtures.

Table 4. FET Mobility (μ), On/Off Current Ratios (I_{on}/I_{off}), and Threshold Voltage (V_T) of the Polymers

polymer	μ (cm^2 V^{-1} s^{-1})	I_{on}/I_{off}	V_T (V)
EH-PCzDCN	2.4×10^{-4}	10^4	−3
EH-PCzDTA	1.1×10^{-3}	10^4	−25
C17-PCzDCN	5.3×10^{-5}	10^3-10^4	−29
C17-PCzDTA	1.5×10^{-4}	10^3-10^4	−13
C17-PCzDDCN	8.8×10^{-5}	10^3-10^4	−14
C17-PCzDDTA	1.6×10^{-4}	10^3-10^4	−6

show very efficient photoresponse from the range of 400−750 nm, and the EH-PCzDCN exhibits the highest EQE (>60%) in the range of 450−550 nm. The shorter alkyl side-chain polymers EH-PCzDCN and EH-PCzDTA demonstrated obviously stronger photoresponse than those of their bulky side chain counterparts and didye-containing polymers, which is consistent with the difference of the J_{sc} values of the solar cell devices based on them. In addition, the integral of the EQEs is consistent with the J_{sc} values measured from the devices.

To understand the cause of variation in solar cell performance, the hole mobility of these polymers was measured using the FET technique under the same conditions. The mobility values and on/off current ratios of the polymers are listed in Table 4. Noticeable, the two shorter alkyl side-chain polymers EH-PCzDCN and EH-PCzDTA exhibit good hole-transporting ability, with mobilities measured to be 2.4×10^{-4} and 1.1×10^{-3} cm^2 V^{-1} s^{-1}, respectively, which are comparable to those reported for promising carbazole-based linear narrow-band gap polymers.[22,30] On the other hand, four bulkier alkyl side-chain polymers show lower hole mobilities (5.3×10^{-5}, 1.5×10^{-4}, 8.8×10^{-5}, and 1.6×10^{-4} cm^2 V^{-1} s^{-1}, respectively) than those of shorter alkyl side-chains polymers. This phenomenon is consistent with that reported by Leclerc, that the nature of the side chain on the N atom of carbazole is crucial for improving the molecular organization of the polymers in thin films and consequently affect the carrier transporting abilities.[52] It was also

(52) Wakim, S.; Aich, B. R.; Tao, Y.; Leclerc, M. *Polym. Rev.* **2008**, *48*, 432–462.

found that the dye content of the polymers has little influence on their carrier transporting properties. The relative low hole mobilites of the polymers with bulkier alkyl side chains may cause the unbalanced transport of charge carriers in the devices, which is consistent with their relative poor FF values obtained in devices, compared to those of EH-PCzDCN and EH-PCzDTA (see Table 3). Thus, the better hole-transporting properties of the shorter alkyl side-chain polymers EH-PCzDCN and EH-PCzDTA are the most likely reasons for their better photovoltaic properties than those of the polymers with bulky alkyl side chains.

Conclusion

In summary, a series of two-dimensional narrow-band gap conjugated polymers based on carbazole bearing different alkyl side chains and dye contents were designed and synthesized. The absorption spectra and band gaps of these polymers could be readily tuned by altering the strength of the pendant acceptor groups and their highest occupied molecular orbital (HOMO) levels could be kept low simultaneously. Significantly enhanced absorption was realized by increasing the dye contents on the conjugated polymer main chains. It was found that the alkyl side chains of the polymers have important influence on the hole-transporting and consequently affect the performance of the resulting devices. All these materials exhibit promising photovoltaic properties, where the highest power conversion efficiency (PCE) value of 4.47% could be achieved based on using EH-PCzDCN as an electron donor. Solar cells based on all of the resultant polymers possess high open-circuit voltage (V_{oc}) values. Considering the flexibility for further chemical modifications of these new type of D-A copolymers, the development of more-efficient materials should be possible by rational selection of appropriate donor moieties in conjugated backbone and pendant acceptor groups for polymer BHJ solar cells applications.

Acknowledgment. The work was financially supported by the Natural Science Foundation of China (No. 50990065, 51010003, 51073058, and 20904011), the Ministry of Science and Technology, China (MOST) National Research Project (No. 2009CB623601) and the Fundamental Research Funds for the Central Universities, South China University of Technology (No.2009220012, 2009220043), the World Class University (WCU) program through the National Research Foundation of Korea under the Ministry of Education, Science and Technology (R31-10035) and the DOE "Future Generation Photovoltaic Devices and Process" program under Project No. DE-FC36-08GO18024/A000. A.K.Y.J. thanks the Boeing−Johnson Foundation for financial support.